RESEARCH ARTICLE

CELL BIOCHEMISTRY & FUNCTION WILEY

MiR-140-5p promotes osteogenic differentiation of mouse embryonic bone marrow mesenchymal stem cells and post-fracture healing of mice

Jianhang Jiao[1] | Guang Feng[2] | Minfei Wu[1] | Yang Wang[1] | Rui Li[3] | Jun Liu[3]

[1]Department of Orthopedics, The Second Hospital of Jilin University, Changchun, China

[2]The Fourth Medical Center of PLA General Hospital, Beijing, China

[3]Department of Hand Surgery, The Second Hospital of Jilin University, Changchun, China

Correspondence
Jun Liu, Department of Hand Surgery, The Second Hospital of Jilin University, No. 218 Ziqiang Street, Nanguan District, Changchun, Jilin 130000, China.
Email: liujun_jliu@163.com

Abstract

MiR-140-5p is high expressed in normal fracture healing, but its specific role and mechanism in tissue-to-bone healing are rarely reported. Therefore, this study investigated the effects of miR-140-5p on tissue-to-bone healing. Clone formation experiment, flow cytometry, Alizarin Red S Staining and Oil Red O Staining were performed to investigate the biological characteristics of mouse embryonic bone marrow mesenchymal stem cells C3H10T1/2. MiR-140-5p mimic was transfected into osteogenic medium (OS)-treated C3H10T1/2 cells to investigate the effects of miR-140-5p on osteogenic differentiation. MiR-140-5p transgenic mouse model and the transgenic fracture model were established, and the effects of miR-140-5p on osteogenic differentiation, bone mineral density (BMD) and bone mass of bone tissues were detected by haematoxylin and eosin staining and computed tomography scan. The expressions of osteocalcin, differentiation-related genes (Runx2, ALP, Spp1 and Bglap3) and miR-140-5p were determined by quantitative real-time polymerase chain reaction. C3H10T1/2 cells showed the abilities of forming cloned differentiation of osteogenesis, fat cells, and its phenotypes including CD44, CD90.1 and Sca-1 but excluding CD45 haematopoietic stem cell marker. Overexpression of miR-140-5p promoted the expressions of differentiation-related genes and calcium deposition of OS-treated C3H10T1/2 cells. MiR-140-5p increased the expression of osteocalcin, BMD and bone mass and promoted bone healing of miR-140-5p-transgenic mice with fracture. MiR-140-5p promoted osteogenic differentiation of mouse embryonic bone marrow mesenchymal stem cells and post-fracture healing in mice.

Significance of the study

C3H10T1/2 cells showed the abilities of forming cloned differentiation of osteogenesis, fat cells and its phenotypes including CD44, CD90.1 and Sca-1 but excluding CD45 haematopoietic stem cell marker. Overexpression of miR-140-5p promoted the expressions of differentiation-related genes and calcium deposition of osteogenic medium-treated C3H10T1/2 cells. MiR-140-5p increased the expression of osteocalcin and bone mineral density and bone mass and promoted bone healing of miR-140-5p-transgenic mice with

fracture. Our results showed that miR-140-5p promoted osteogenic differentiation of mouse embryonic bone marrow mesenchymal stem cells and post-fracture healing in mice, which may be a therapeutic target for treating fractures and promoting bone healing.

KEYWORDS

bone healing, C3H10T1/2 cells, fracture, miR-140-5p, osteogenic differentiation

1 | INTRODUCTION

Bone fracture is one of the most frequent injuries in the musculoskeletal system,[1] and its causes are complex and the types of fractures are diverse.[2,3] Despite the strong healing capacity of bones, 5%-10% of fracture patients experience a certain degree of disturbance during healing, leading to delayed healing of fractures or nonunion, thus causing physical discomfort to the patients.[4] Therefore, studying the physiological process of fracture healing and its regulatory mechanism will be helpful to promoting fracture healing.

The differentiation, maturation and activity of osteoblasts involve a variety of hormones and cytokines that mediate the regulation of differentiation-related gene expressions via different signal transduction pathways, and the maintenance of osteoblast differentiation and activity plays a crucial role in fracture healing.[5] In recent years, MicoRNAs (miRNAs)-mediated post-transcriptional regulation has been found to inhibit cellular protein expression and considered to be an important intracellular regulatory pathway in a wide range of life processes.[6-8] Besides, studies have found that miRNAs, as important regulators, are involved in various complex links of osteoblast differentiation and bone formation.[9,10] It has been reported that miR-133, miR-135, miR-29, miR-141 and miR-200a inhibit the differentiation of osteoblasts through regulating key proteins in osteoblast differentiation.[11-13] Studies confirmed the role of miR-214 in inhibiting bone formation in three animal models of miR-214 transgenic mice, oariectomized mice and hindlimb deloading mice. in vitro cell experiments have found that miR-214 inhibits osteoblastic activity after transcriptional expression.[14] So far, however, few studies have reported the mechanism of miRNAs in osteoblast differentiation and activity in fracture healing. What's more, miR-140-5p has been reported to be high expressed in healing fractures compared with unhealed fractures,[15] but its specific role and mechanism in fractures are rarely reported.

Therefore, this study further explored the role and mechanism of miR-140-5p in bone healing after fracture by transfecting miR-140-5p into osteoblasts to detect cell biological functions and mineralisation. Moreover, a transgenic fracture mouse model was established to detect changes in bone density and bone mass in mice.

2 | METHODS

2.1 | Cell culture

Mouse Embryonic Bone Marrow Mesenchymal Stem Cells C3H10T1/2 were obtained from Cell Bank of Shanghai Institutes for Biological Sciences, Chinese Academy of Sciences. All the cells were cultured in Dulbecco's modified Eagle's medium (DMEM) cell culture medium containing 10% foetal bovine serum (FBS, Gibco, USA), 100 mg/mL streptomycin and 100 U/mL penicillin (15 140 163, Thermo Fisher Scientific) in a 5% CO_2 atmosphere at 37°C. After the cells were cultured 14 days, colony formation assay was used to observe the colony formation, an optical microscope (CKX31, Olympus, Japan) was used to observed the cell morphology. Moreover, Alizarin red S and Oil Red O staining were used to analyse the pluripotent differentiation of cells. After Alizarin red S, if the cells have calcium nodules, it proves that the cells are induced to osteoblasts. After Oil Red O staining, if the cells have fat particles, it proves that the cells are induced to adipocytes.

2.2 | Transfection

A culture medium (2 mL) containing 2×10^5 C3H10T1/2 cells was added into each well of a 6-well plate and the plate was then placed in an incubator to culture the cells at 37°C until they reached 60% confluence. Next, A and B transfection solution were prepared. A solution was prepared by dissolving 20 pmol of miR-140-5p mimic (Shanghai GenePharma Co., Ltd., China) in 50 μL of DMEM (Hyclone, USA), whilst B solution was prepared by dissolving 1 μL of Lipofectamine2000 (Invitrogen, USA) in 50 μL of DMEM. Then, the two solutions were thoroughly mixed and stood for 5 minutes. The mixture was then added to the medium at 37°C and held for 24 hours. The sequence of miR-140-5p mimic was CAGUGGUUUUACCCUAUGGUAG.

2.3 | Colony formation assay

After transfection, digestion and cell counting, the cells were cultured in 12-well plates at 100 cells per well at 37°C in a 5% CO_2 atmosphere for 3 weeks, and the conditioned medium was changed every 3 days (d) to observe clone formation. The culture was terminated when the cloned cells were within 50-150 fields, and then the medium was discarded, and the cells were rinsed twice in Dulbecco's Phosphate Buffered Saline (DPBS, D8662, Sigma-Aldrich, USA). Next, 1 mL of methanol (34 860, Sigma-Aldrich, USA) was added into each well to fix the cells for 15 minutes, and 1 mL of giemsa (999D715, Thermo Fisher Scientific, USA) was added into each well and held for 30 minutes. Colony formation rate was calculated by the following equation: colony formation rate = (number of colonies/number of seeded cells) × 100%. Each treatment was carried out in triplicate.

2.4 | Alizarin red S

After culturing C3H10T1/2 cells in osteogenic medium (50 μmol of ascorbic acid, 10 mmol of β-glycerol phosphate and 100 nmol of dexamethasone were added to α-MEM culture medium containing 10% FBS), Alizarin Red Staining was performed using an Alizarin Red S Staining Kit (ST1078-25g, Beyotime Biotechnology, China). According to the protocol, the cells were washed with 1 mL of phosphate buffer saline (PBS) twice, and then fixed with 4% paraformaldehyde in PBS for 15 minutes at room temperature. Before staining, the fixation fluid was removed and the cells were washed with diH$_2$O for three times. After removing diH$_2$O, 1 mL of 2% Alizarin Red S Stain solution was added into each well and incubated with the cells for 20 minutes at room temperature. Then the solution was removed and the cells were washed with diH$_2$O for 3 times. Next, 1 mL of diH$_2$O was added into each well to prevent the cells from drying. The samples were then observed under the optical microscope (CKX31, Olympus, Japan).

2.5 | Oil Red O staining

HG-DMEM culture medium containing FBS (10%) was configured and 1 μM dexamethasone, 10 μg/mL insulin, 200 μM indomethacin and 0.5 mM IBMX were added to the medium. C3H10T1/2 cells were cultured in adipogenic medium and lipid droplets were observed by Oil Red O staining. Then, 0.05 g of Oil Red O powder (00625, Sigma-Aldrich, USA) was added into 99% propanediol (30157018, Sinopharm Chemical Reagent Beijing Co., Ltd, http://www.crc-bj.com/Products.aspx?, China) to prepare Oil Red O dyes. After removing C3H10T1/2 cell culture medium, the cells were washed with 1 mL of PBS twice. Then the cells were fixed with 4% paraformaldehyde in PBS for 15 minutes at room temperature. Afterwards, the solution was removed and the cells were washed with diH$_2$O for three times. After that, 0.5% Oil Red O was added to incubate the cells for 1 hour and then the cells were washed with 70% ethanol for three times. Finally, an optical microscope was used to observe the pathological changes.

2.6 | Flow cytometry assay

To determine the surface phenotypes of C3H10T1/2 cells, the cells were suspended in 100 μL of PBS and a 1×10^6/mL cell suspension was prepared. Then 100 μL of the cell suspension was incubated with fluorochrome-conjugated primary antibodies against Sca-1 (ab25031, Abcam, USA), CD90.1 (205 903, Biolegend, USA), CD44 (103 011, Biolegend, USA), and CD45 (103 111, Biolegend, USA) for 30 minutes, followed by incubation with phocein isothiocyanate-labelled goat anti-mouse secondary antibody (406 001, Biolegend, USA) at room temperature in the dark for 30 minutes. The stained cells were subjected to flow cytometry analysis.

2.7 | Ethics statement

The animal experiments in this study were approved by the animal ethics committee of the Second Hospital of Jilin University (TSHJU20181105) and were in accordance with the guidelines of the National Institutes of Health (USA) for animal experiments.

2.8 | Establishment of transgenic mouse model and fracture model

A total of 32 6-week-old male BALB/c mice were obtained from CAVENS, Changzhou, China. The mice were divided into four groups (n = 8), namely, model group, model+miR-140-5p group (miR-140-5p transgenic mice construction), fracture model group and fracture model+miR-140-5p group.

For constructing of miR-140-5p transgenic mice: the miR-140-5p sequence was synthesized, and surface plasmids containing preserved osteocalcin initiators were obtained by Sall and EcoR I double enzyme digestion, and DNA gel recovery kit was used to retract linear carrier fragments. The linearized plasmid was connected to the synthesized miR-140-5p sequence overnight at 16°C. Sensitive thin *Escherichia coli* DH5α strain was prepared, the junction product was transformed into DH5α sensitive cells, and the reassembly vector was screened. The white resistant colonies were amplified, the plasmids were extracted, and the recombinant plasmids were identified by Sall and EcoR I restriction endonuclease. The miR-140-5p plasmids normally expressed in mouse cells were sent to Guangzhou Saiye Biotechnology Co., Ltd. for pronuclei microinjection, and the bone tissue-specific high-expressed miR-140-5p and transgenic mouse models were generated. In this study, we injected the constructed miR-140-5p expression plasmid into the pronucleus of fertilized eggs of C57BL/6 mice by fibre injection. Three weeks after the mouse was born, polymerase chain reaction (PCR) was used to identify whether the expression plasmid was integrated into the genome of the newborn mouse. In this experiment, a total of 50 mice were born after microinjection of miR-140-5p expression plasmid embryos, and 16 mice were successfully overexpressed by PCR.

In the fracture model and fracture model+miR-140-5p groups (fracture model), after the mice were narcotized by intraperitoneal injection of 65 mg/kg pentobarbital for 1 hour, a 10 mm incision was made on the right thigh of the mice. Then, the vastus lateralis and hamstring muscles were separated to expose the femur. Next, the central shaft of the femur was amputated by osteotomy. Then 25 needles were placed into the intramedullary canal of the femoral condyle in a retrograde fashion to fix the severed femur. Muscle septum and skin incisions were closed by absorbable sutures. The mice were sacrificed at week 6 to observe the bone callus reconstruction. Computed tomography (CT) was used to evaluate femora of the mice with fracture through measuring bone mineral density (BMD), volume of high density bone (BV$_h$, mm^3), total tissue volume (TV, mm^3), volume of low density bone (BV$_l$, mm^3), total bone volume

$(BV_t, = BV_h + BV_l)$, and their proportions were normalized to the tissue volumes $(=BV_h/TV, BV_l/TV, BV_t/TV)$.

2.9 | Quantitative reverse transcription-polymerase chain reaction (qRT-PCR)

Total RNAs were extracted from tissues or cells using Trizol reagent (12183555, Thermo Fisher Scientific, USA), and NanoDrop One/OneC micro-UV-visible spectrophotometer (ND-ONEC-W, Thermo Scientific, USA) was used to measure RNA concentration, which was then adjusted to 500 ng/µL for subsequent experiments. Then, RNAs were reverse-transcribed into cDNAs using a PrimeScript RT kit (RR037A, Takara, China). The miRNA expression levels were determined using a SuperScript III Platinum SYBR Green One-Step qRT-PCR Kit (11736059, Thermo Fisher Scientific, USA). U6 served as an internal reference. The ABI7500 system (Applied Biosystems) was used in a qRT-PCR reaction, and $2^{-\Delta\Delta CT}$ method was used to calculate multiple changes in relative mRNA expression levels.[16] One microlitres of distilled water, 3 µL of cDNA, 5 µL of DNA polymerase, and 1 µL of primer were thoroughly mixed together. The PCR cycle program was set as follows: at 95°C for 10 minutes, at 95°C for 15 seconds, at 72°C for 15 seconds, for a total of 40 cycles. All primer sequences used for qRT-PCR in this study were listed in Table 1.

2.10 | Haematoxylin and eosin (HE) staining

HE staining was performed on the bone tissues of mice. Briefly, after being fixed with formaldehyde for 24 hours, the tissues were dehydrated with gradient alcohol, transparentized with xylene, embedded in paraffin and sectioned into 5 µm slices. Then, the sections were stained with haematoxylin for 20 minutes, and placed in

TABLE 1 Primer sequences and products size for polymerase chain reaction

Gene	Sequence (5′ to 3′)
miR-140	Forward: CGTATCCAGTGCAATTGCCG
	Reverse: GTCGTATCCAGTGCGTGCG
Runx2	Forward: CATCCCCATCCATCCACTCC
	Reverse: GCCAGAGGCAGAAGTCAGAG
ALP	Forward: ACCCGAAGAACAGAACCGAC
	Reverse: TGCGGTTCCAGACATAGTGG
Spp1	Forward: CTGGCAGCTCAGAGGAGAAG
	Reverse: TTCTGTGGCGCAGGACATT
Bglap3	Forward: CAAGCAGGAGGGCAATAAGGT
	Reverse: AGCAGGGTCAAGCTCACATAG
GAPDH	Forward: ATACGGCTACAGCAACAGGG
	Reverse: GCCTCTCTTGCTCAGTGTCC

acidification solution (1% hydrochloric acid in 75% ethanol) for 1 minute to remove cytoplasm blue, and then rinsed in tap water for 10 minutes. Next, the tissue sections were stained with eosin for 15 minutes. Afterwards, the sections were dehydrated in 100% ethanol for 15 minutes, and then transparentized with xylene for 15 minutes. Finally, neutral gum was used to seal the film, and the pathological changes of rat aortic tissues were observed under an optical microscope (CKX31, Olympus, Japan).

2.11 | Statistical analysis

SPSS 18.0 (Chicago, USA) was used to analyse the data. In this study, the data were shown as mean ± SD. Differences between more than two groups were compared by ANOVA, whilst differences between two groups were compared by t test. Each experiment was performed in triplicate. $P < .05$ was defined as statistically significant.

3 | RESULTS

3.1 | Characteristics of mouse embryonic mesenchymal stem cells (C3H10T1/2)

We first detected the biological characteristics of C3H10T1/2 cells, and the results showed that C3H10T1/2 cells could form clones (Figure 1A), at the same time, as shown in Figure 1B, after Alizarin Red S, the cells had calcium nodules compared to the BMSC group, indicating that the cells were induced as osteoblasts. After oil red O staining, there were fat particles in the cells compared to the BMSC group, which proved that the cells were induced as adipocytes. Then, the phenotype of C3H10T1/2 cells was detected by flow cytometry, and the results showed that the phenotypes included CD44, CD90.1 and Sca-1 but excluded CD45 haematopoietic stem cell marker (Figure 1C).

3.2 | Effects of miR-140-5p on osteogenic differentiation of C3H10T1/2 cells

The transfection rate of miR-140-5p in C3H10T1/2 cells was determined by qRT-PCR, and the results showed that miR-140-5p was high expressed in the cells after the transfection ($P < .001$, Figure 2A). The cells were then cultured in OS for 3 days, and the expressions of osteogenic differentiation-related genes were detected by qRT-PCR, and the results showed that overexpressed miR-140-5p promoted OS-induced expressions of osteoblast differentiation-related genes (Runx2, ALP, Spp1 and Bglap3) ($P < .05$, $P < .001$, Figure 2B). Calcium deposition was determined by Alizarin Red S staining after the cells were treated with miR-140-5p mimic and OS, and the results demonstrated that overexpressed miR-140-5p promoted calcium deposition in OS-treated C3H10T1/2 cells ($P < .05$, $P < .001$, Figure 2C).
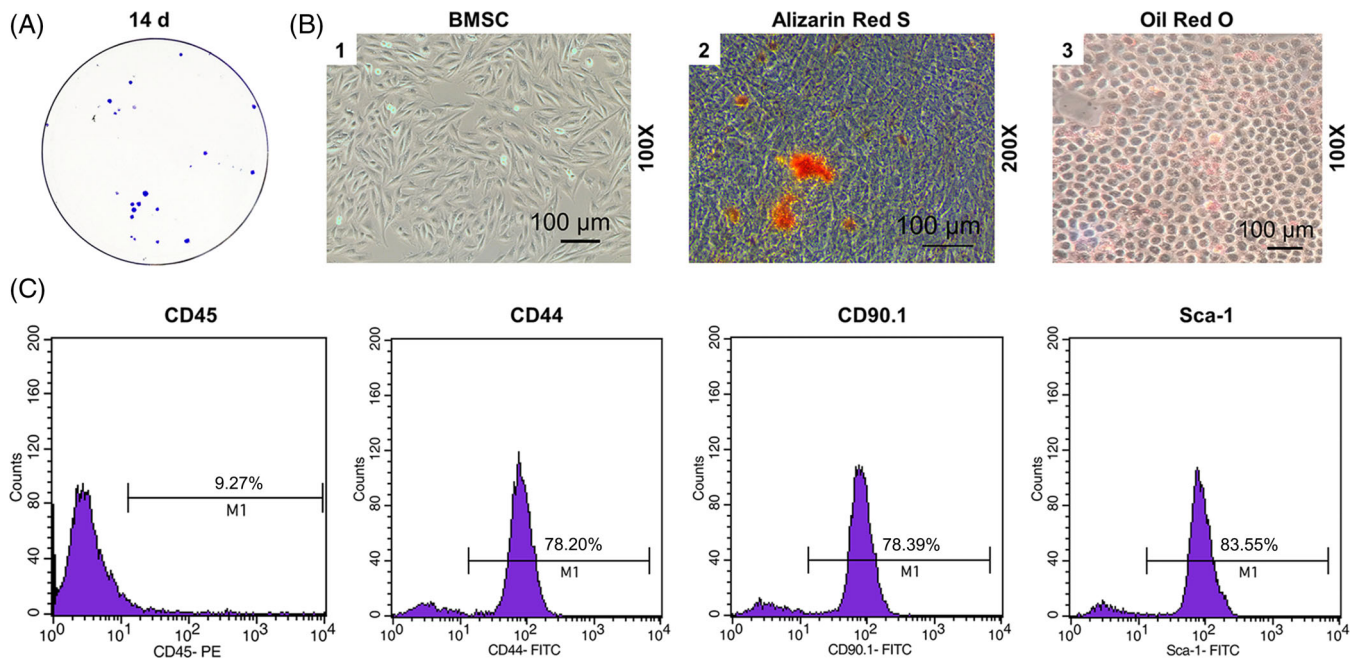
FIGURE 1 Characterisation of mouse embryonic mesenchymal stem cells (C3H10T1/2). (A) The number of C3H10T1/2 cells was counted in the cloning experiment. (B) Alizarin Red S staining was used to observe the osteogenic differentiation of C3H10T1/2 cells, and Oil Red O staining was used to observe the adipogenesis of the cells. (C) The expressions of CD45, CD44, CD90.1 and sca-1 in C3H10T1/2 cells were detected by flow cytometry

3.3 | Expression of miR-140-5p in transgenic mice and its effects on bone differentiation in mice with fracture

The transgenic mouse model of miR-140-5p was established, and the expression of miR-140-5p in bone, lung, brain, heart, spleen, liver, fat and skeletal muscle tissues was detected by qRT-PCR. The data demonstrated that miR-140-5p was highly and specifically expressed in the bones of modelled mice ($P < .001$, Figure 3). In the fracture models of wild-type, miR-140-5p and transgenic mice, histological examinations were performed at the fracture site 7, 14 and 21 days after fracture to observe the effects of miR-140-5p-specific expression in bone tissue during fracture healing. The results showed that in wild-type mice, a large amount of granulation tissue could be seen at the broken end 7 days after fracture, and calluses were not obvious. However, more fibrous and cartilaginous calluses, and some calcified and large callus were observed on day 21, and some of the calluses were connected into pieces and woven into bone. In miR-140-5p transgenic mice, fewer fibrous and cartilaginous calluses could be seen 7 days after fracture, and a large number of calcified calluses could be seen 14 days after fracture; moreover, calcified calluses were connected 21 days after fracture, and the woven bone was connected into pieces, and the medullary cavity began to form (Figure 4A). The expression of Osteocalcin was detected by qRT-PCR 7, 14 and 21 days after fracture, and the results showed that miR-140-5p promoted the expression of osteocalcin in fracture model mice ($P < .05$, $P < .001$, Figure 4B). In addition, BMD and bone mass of fractured mice were calculated by CT scan. As shown in Table 2, the BMD and bone mass of miR-140-5p transgenic mice with fracture were significantly higher than those of the control group and the fracture model group ($P < .05$, $P < .001$).

4 | DISCUSSION

After bone injury, in addition to orderly regulation of growth factors, the migration, proliferation and other functional roles of various repair cells are key to obtain an ideal result of bone repair.[17-19] Bone marrow mesenchymal stem cells adhere to bone marrow stromal cells and have the potential to self-renew and differentiate into bone, cartilage, fat and muscle cell lines.[20] Studies have found that C3H10T1/2 cells are undifferentiated mouse embryonic mesenchymal stem cells characterized by having a strong proliferation ability and multi-directional differentiation potential, and they can differentiate into adipocytes, osteoblasts and chondrocytes under certain conditions.[21,22] In this study, we studied the characteristics of C3H10T1/2 cells, and the results showed that the formed cell colonies were visible 14 days after culture. CD44, CD90.1, and Sca-1 are important surface markers for bone marrow mesenchymal stem cells.[23] BMSCs are non-haematopoietic cells and do not express CD45.[24] In this study, the expressions of CD44, CD90.1 and Sca-1, rather than that of CD45, were detected by flow cytometry, indicating that C3H10T1/2 cells are not bone marrow haematopoietic cells but bone marrow mesenchymal stem cells. In addition, our research found that C3H10T1/2 cells could differentiate into osteoblasts and adipocytes.
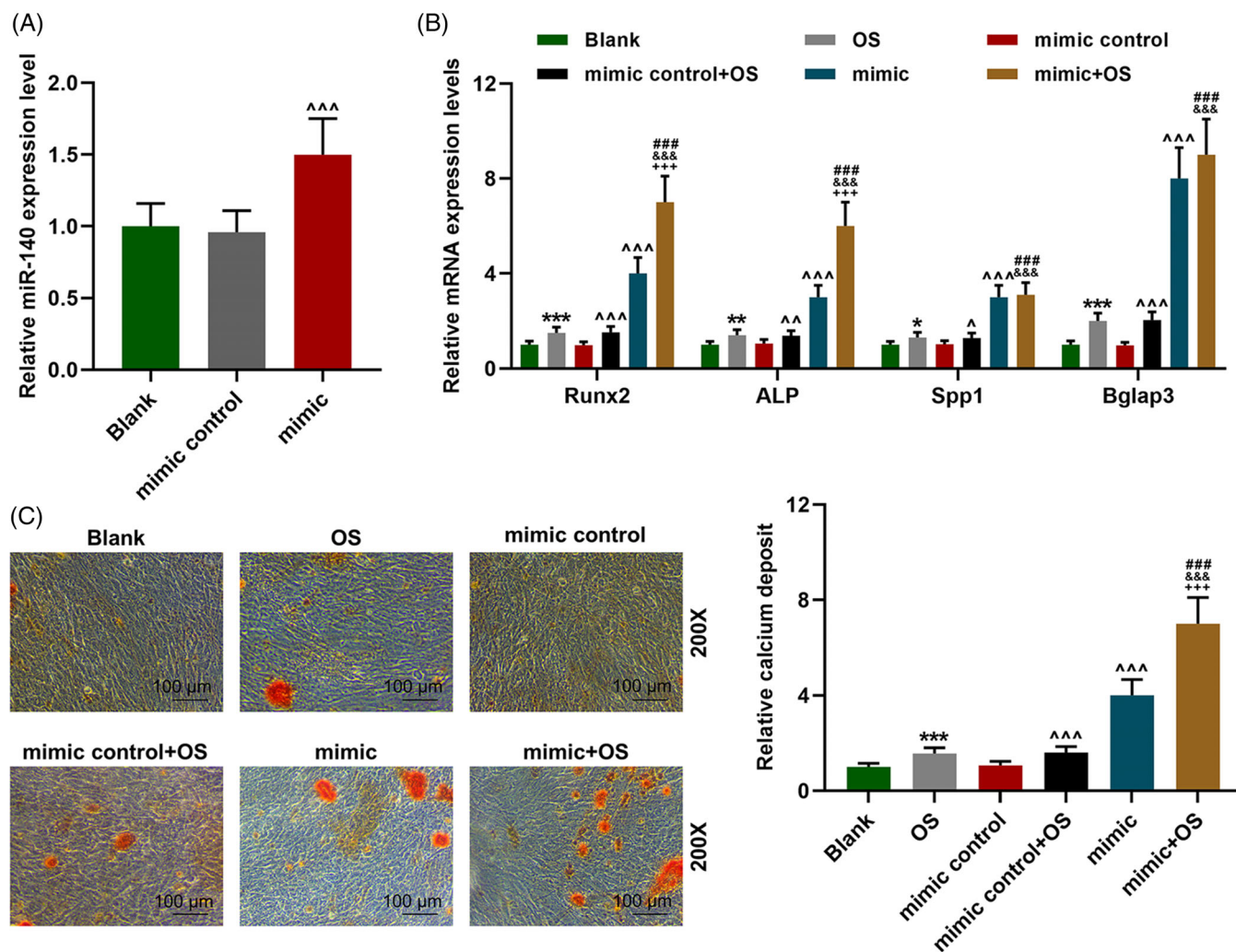
FIGURE 2 Effects of miR-140-5p on the osteogenic differentiation of C3H10T1/2 cells. (A) The conversion rate of miR-140-5p in C3H10T1/2 cells was detected by qRT-PCR. (B) The cells were cultured in OS for 3 days, and the expressions of osteogenic differentiation-related genes were detected by qRT-PCR. (C) Calcium deposition was determined by Alizarin Red S staining after the cells were treated with miR-140-5p mimic and OS. $^*P < .05$, $^{**}P < .01$, $^{***}P < .001$, vs Blank; $^\wedge P < .05$, $^{\wedge\wedge}P < .01$, $^{\wedge\wedge\wedge}P < .001$, vs mimic control; $^{\#\#\#}P < .001$, vs OS; $^{\&\&\&}P < .001$, vs mimic control + OS; $^{+++}P < .001$, vs mimic

Several studies have shown that miRNAs play an important role in the differentiation of mesenchymal stem cells into osteoblasts. For example, overexpression of miR-140-5p can promote the differentiation of bone marrow mesenchymal stem cells into chondrocytes.[25] Therefore, C3H10T1/2 cells were used as the research objects to explore the effect of miR-140-5p on osteogenic differentiation. Runx2 is an osteogenesis-specific transcription factor that plays a vital role in the development, differentiation and bone formation of osteoblasts, and its expression can be regulated by a variety of miRNAs[26,27]; ALP is a marker for early cell differentiation and is related to bone cell synthesis before bone calcification,[28] and overexpressed miR-615-3p can inhibit ALP expression[29]; Spp1 is a late marker for osteoblasts and is closely related to bone matrix mineralisation; Bglap is a signature enzyme of osteoblasts. Studies found that the differential expressions of miR-29b, miR-30c2 and miR-125b are closely related to Spp1 and Bglap.[30] In this study, we investigated the effects of miR-140-5p on

the expressions of Runx2, ALP, Spp1 and Bglap in C3H10T1/2 cells, and the data demonstrated that overexpressed miR-140-5p can promote the expressions of osteogenesis-related genes. At the same time, by staining calcified nodules on C3H10T1/2 cells, we also confirmed that overexpression of miR-140-5p can promote osteogenic differentiation of cells. Therefore, miR-140-5p can regulate the differentiation of C3H10T1/2 cells into bone, which is consistent with the findings of Mahboudi et al[25] Moreover, we speculated that miR-140-5p was closely related to bone healing.

Murata et al found that inhibition of miR-92a expression in mice with fracture can promote bone healing by promoting angiogenesis.[31] In order to further investigate the effect of miR-140-5p on fracture healing, we transfected miR-140-5p overexpression vector into mice, and found that miR-140-5p was specifically overexpressed in the bone of transgenic mice. Then, a fracture model was established in mice and transgenic fracture models. Through histopathological
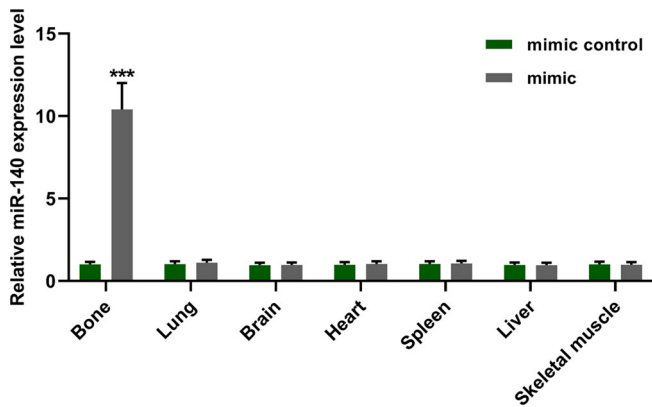
FIGURE 3 Expression of miR-140-5p in transgenic mice. The transgenic mouse model of miR-140-5p was established, and the expressions of miR-140-5p in the bone, lung, brain, heart, spleen, liver, fat and skeletal muscle tissues were detected by qRT-PCR. $^{***}P < .001$, vs mimic control. 16 BALB/c mice were used and eight in each group

observation, we found that 21 days after the mice with fracture were transfected with miR-140-5p, there were a large number of calcified nodules at the fracture site of the mice, and braved bones joined into slices, and medullary cavities began to form. At the same time, the BMD and bone mass of the fractured mice were calculated, and the results showed that the mice transfected with miR-140-5p had higher bone density and bone mass than those in the fractured model group. Therefore, miR-140-5p is involved in the physiological process of mice with fracture and promotes bone healing. Moreover, rescue experiments will be conducted to further verify our results in our future studies.

In conclusion, miR-140-5p promoted osteogenic differentiation of mouse embryonic bone marrow mesenchymal stem cells and post-fracture healing in mice, which may be a therapeutic target for treating fractures and promoting bone healing. However, we still need to perform experiments to further reveal the molecular regulatory mechanism of miR-140-5p in promoting bone healing.
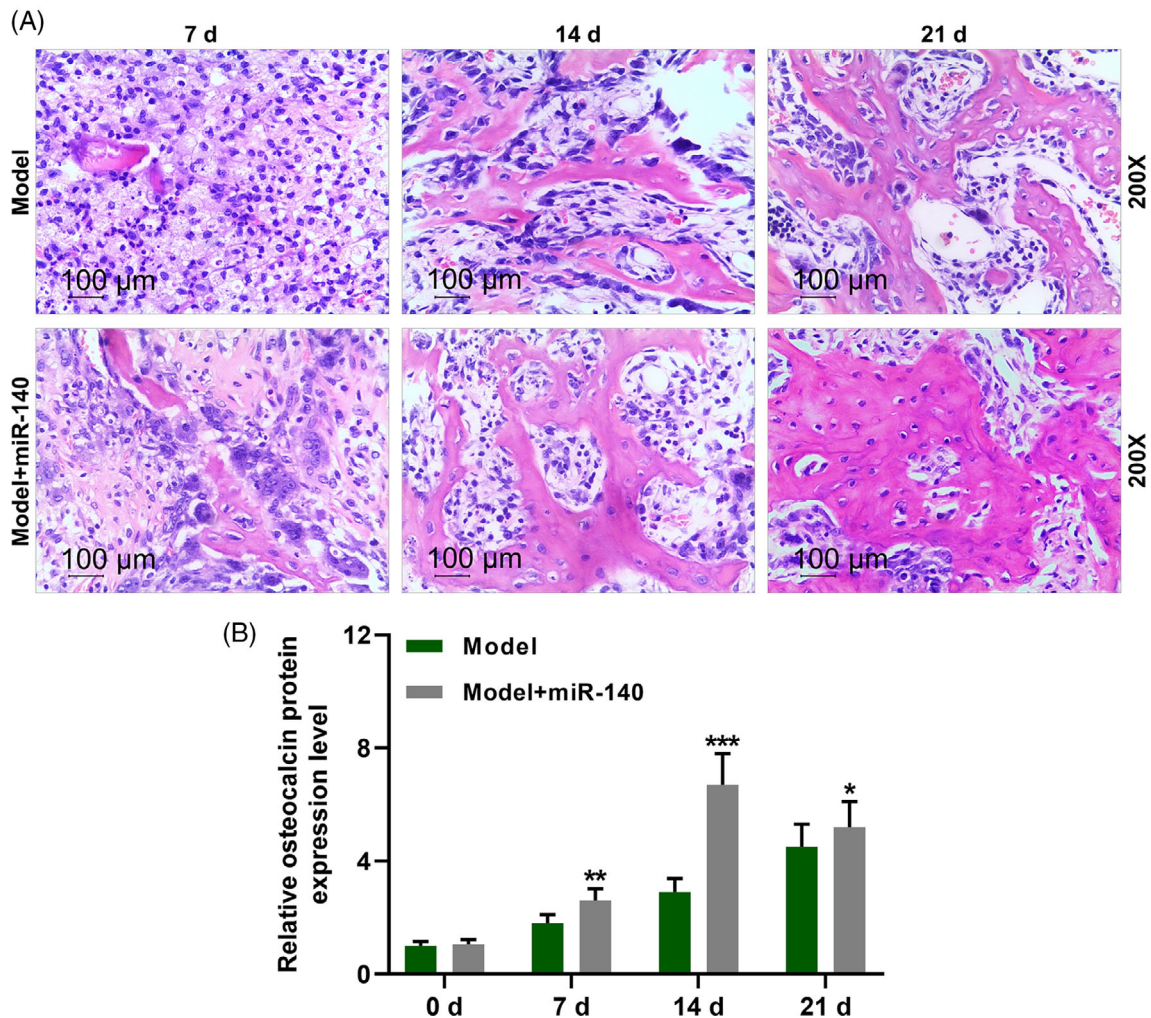

FIGURE 4 Effect of miR-140-5p on bone differentiation in fractured mice. (A) A fracture mouse model was established. After 7, 14 and 21 days of fracture, HE staining was used to observe the effects of miR-140-5p on the physiological changes of the fracture site. (B) Osteocalcin expression was detected by qRT-PCR on day 7, 14 and 21 after fracture. $^*P < .05$, $^{**}P < .01$, $^{***}P < .001$, vs Model. 16 BALB/c mice were used and eight in each group

TABLE 2 Comparison of bone mineral density and bone mass in fractured mice and transgenic mice

Parameter	Model	Model+miR-140	t	P
TV (mm^3)	20.63 ± 3.81	18.35 ± 3.54	1.164	.267
BV$_t$ (mm^3)	16.50 ± 3.56	13.74 ± 3.05	1.556	.146
BV$_h$ (mm^3)	9.11 ± 1.90	8.78 ± 1.23	0.379	.711
BV$_1$ (mm^3)	6.89 ± 2.32	5.57 ± 1.33	1.304	.217
BV$_t$/TV (%)	83.29 ± 17.17	77.19 ± 12.50	0.760	.462
BV$_h$/TV (%)	43.55 ± 2.45	49.43 ± 5.74	−2.493	.028
BV$_1$/TV (%)	34.76 ± 5.39	31.61 ± 2.10	1.441	.175
BMD (mg HA/ccm)	421.04 ± 85.90	474.85 ± 17.21	−3.329	.006

Abbreviations: BMD, bone mineral density of callus; BV$_t$, total bone volume; BV$_h$, volume of high density bone; BV$_1$, volume of low density bone; TV, total tissue volume.

$P < .05$ is statistically significant.

CONFLICT OF INTEREST

The authors declare no potential conflict of interest.

DATA AVAILABILITY STATEMENT

Data sharing is not applicable to this article as no new data were created or analyzed in this study.

ORCID

Jianhang Jiao   https://orcid.org/0000-0001-9975-9110

Jun Liu   https://orcid.org/0000-0002-7106-1359

REFERENCES

1. Ono T, Takayanagi H. Osteoimmunology in bone fracture healing. *Curr Osteoporos Rep*. 2017;15(4):367-375.
2. Care W, Arnautou P, Segot A, et al. Fracture of unusual cause. *La Revue de Medecine Interne*. 2018;39(8):665-666.
3. Peddada KV, Sullivan BT, Margalit A, Sponseller PD. Fracture patterns differ between Osteogenesis Imperfecta and routine pediatric fractures. *J Pediatr Orthop*. 2018;38(4):e207-e212.
4. Nelson FR, Brighton CT, Ryaby J, et al. Use of physical forces in bone healing. *J Am Acad Orthop Surg*. 2003;11(5):344-354.
5. Claes L, Recknagel S, Ignatius A. Fracture healing under healthy and inflammatory conditions. *Nat Rev Rheumatol*. 2012;8(3):133-143.
6. Choi SY, Pang K, Kim JY, et al. Post-transcriptional regulation of SHANK3 expression by microRNAs related to multiple neuropsychiatric disorders. *Mol Brain*. 2015;8(1):74.
7. Han YC, Vidigal JA, Mu P, et al. An allelic series of miR-17 approximately 92-mutant mice uncovers functional specialization and cooperation among members of a microRNA polycistron. *Nat Genet*. 2015; 47(7):766-775.
8. Khandal H, Parween S, Roy R, Meena MK, Chattopadhyay D. MicroRNA profiling provides insights into post-transcriptional regulation of gene expression in chickpea root apex under salinity and water deficiency. *Sci Rep*. 2017;7(1):4632.
9. Li H, Xie H, Liu W, et al. A novel microRNA targeting HDAC5 regulates osteoblast differentiation in mice and contributes to primary osteoporosis in humans. *J Clin Invest*. 2009;119(12):3666-3677.
10. Xia ZY, Hu Y, Xie PL, et al. Runx2/miR-3960/miR-2861 positive feedback loop is responsible for Osteogenic Transdifferentiation of vascular smooth muscle cells. *Biomed Res Int*. 2015;2015:624037.
11. Panizo S, Naves-Diaz M, Carrillo-Lopez N, et al. MicroRNAs 29b, 133b, and 211 regulate vascular smooth muscle calcification mediated by high phosphorus. *J Am Soc Nephrol*. 2016;27(3): 824-834.
12. Qiu W, Kassem M. miR-141-3p inhibits human stromal (mesenchymal) stem cell proliferation and differentiation. *Biochim Biophys Acta*. 2014;1843(9):2114-2121.
13. Itoh T, Nozawa Y, Akao Y. MicroRNA-141 and -200a are involved in bone morphogenetic protein-2-induced mouse pre-osteoblast differentiation by targeting distal-less homeobox 5. *J Biol Chem*. 2009;284 (29):19272-19279.
14. Wang X, Guo B, Li Q, et al. miR-214 targets ATF4 to inhibit bone formation. *Nat Med*. 2013;19(1):93-100.
15. Takahara S, Lee SY, Iwakura T, et al. Altered expression of microRNA during fracture healing in diabetic rats. *Bone Joint Res*. 2018;7(2): 139-147.
16. Livak KJ, Schmittgen TD. Analysis of relative gene expression data using real-time quantitative PCR and the 2(−Delta Delta C [T]) method. *Methods*. 2001;25(4):402-408.
17. Degano IR, Vilalta M, Bago JR, et al. Bioluminescence imaging of calvarial bone repair using bone marrow and adipose tissue-derived mesenchymal stem cells. *Biomaterials*. 2008;29(4):427-437.
18. Bruder SP, Fink DJ, Caplan AI. Mesenchymal stem cells in bone development, bone repair, and skeletal regeneration therapy. *J Cell Biochem*. 1994;56(3):283-294.
19. Rana D, Kumar S, Webster TJ, Ramalingam M. Impact of induced pluripotent stem cells in bone repair and regeneration. *Curr Osteoporos Rep*. 2019;17(4):226-234.
20. Hu K, Sun H, Gui B, Sui C. TRPV4 functions in flow shear stress induced early osteogenic differentiation of human bone marrow mesenchymal stem cells. *Biomed Pharmacother*. 2017;91:841-848.
21. Makhijani NS, Bischoff DS, Yamaguchi DT. Regulation of proliferation and migration in retinoic acid treated C3H10T1/2 cells by TGF-beta isoforms. *J Cell Physiol*. 2005;202(1):304-313.
22. Bobick BE, Cobb J. Shox2 regulates progression through chondrogenesis in the mouse proximal limb. *J Cell Sci*. 2012;125 (Pt 24): 6071-6083.
23. Nadri S, Soleimani M, Hosseni RH, Massumi M, Atashi A, Izadpanah R. An efficient method for isolation of murine bone marrow mesenchymal stem cells. *Int J Dev Biol*. 2007;51(8):723-729.
24. Fu Q, Zhang Q, Jia LY, et al. Isolation and characterization of rat Mesenchymal stem cells derived from granulocyte Colony-stimulating factor-mobilized peripheral blood. *Cells Tissues Organs*. 2015;201(6): 412-422.
25. Mahboudi H, Soleimani M, Hanaee-Ahvaz H, et al. New approach for differentiation of bone marrow Mesenchymal stem cells toward chondrocyte cells with overexpression of MicroRNA-140. *ASAIO J*. 2018;64(5):662-672.
26. Ji Q, Xu X, Xu Y, et al. miR-105/Runx2 axis mediates FGF2-induced ADAMTS expression in osteoarthritis cartilage. *J Mol Med*. 2016;94 (6):681-694.

27. Eguchi T, Watanabe K, Hara ES, Ono M, Kuboki T, Calderwood SK. OstemiR: a novel panel of microRNA biomarkers in osteoblastic and osteocytic differentiation from mesencymal stem cells. *PLoS One.* 2013;8(3):e58796.

28. Mirakbari SM. Proposal for a new mechanism of action for aluminum phosphide (ALP) for causing local injuries in ALP poisoning: should treatment strategies be modified? *Hum Exp Toxicol.* 2016;35(10):1145-1146.

29. Yin J, Zhuang G, Zhu Y, et al. MiR-615-3p inhibits the osteogenic differentiation of human lumbar ligamentum flavum cells via suppression of osteogenic regulators GDF5 and FOXO1. *Cell Biol Int.* 2017;41(7):779-786.

30. Laxman N, Rubin CJ, Mallmin H, et al. Global miRNA expression and correlation with mRNA levels in primary human bone cells. *RNA.* 2015;21(8):1433-1443.

31. Murata K, Ito H, Yoshitomi H, et al. Inhibition of miR-92a enhances fracture healing via promoting angiogenesis in a model of stabilized fracture in young mice. *J Bone Miner Res.* 2014;29(2):316-326.